



Microscopic Mechanism of the High-Temperature Strength Behaviour of a C/SiC Composite

Fei Su¹ · Pengfei Huang²

Received: 18 February 2019 / Accepted: 6 March 2019 / Published online: 16 March 2019
© Springer Nature B.V. 2019

Abstract

In this paper, a high-temperature test experimental system is built to investigate the dependence of the strength of a C/SiC composite material on temperature. Unintuitively, the strength increases with temperature. To investigate the microscopic mechanism, scanning electron microscopy (SEM) of an in situ bending test experiment is performed. Our hypothesis is that due to significant residual tensile stress in inter-fibre matrix, external loads reach the ultimate stress first. As the temperature increases, the matrix residual tensile stress decreases, a larger external load needs to be applied for matrix failure, which is exhibited macroscopically as increased strength. To prove this hypothesis, the inter-fibre matrix residual stress and its dependence on temperature are calculated via a finite element method. Next, using a SiC wrapper layer around a single C fibre as an experiment object, the finite element calculation is verified directly via micro-Raman spectroscopy.

Keywords C/SiC composite material · Strength · Residual stress · Micro-Raman spectroscopy

1 Introduction

C/SiC composites are normally produced under a vacuum at high temperatures of approximately 1000 °C via chemical vapour infiltration (CVI) [1–3]. These materials have advantages such as low density, high strength and a low thermal expansion coefficient [4, 5]. Recently, they have become an important high-temperature structural material in aviation and aerospace [6], where they are commonly used as materials for high-speed aircraft missile stabilizer wings and gas turbine thermal section components [7]. Therefore, understanding the high-temperature mechanical properties and underlying microscopic mechanisms of these materials is greatly important to improving the manufacturing process for this material and fully leveraging its material efficiency.

✉ Fei Su
sufei@buaa.edu.cn

¹ School of Aeronautical Science and Engineering, Beihang University, Beijing, China

² Chinese Academy of Space Technology(Xi'an), Xi'an, China

According to some reports, the strength of these materials increased with temperature [8–10]. To explain this unusual phenomenon, some researchers suggested that as the temperature increased, interior residual stress was released, which led to macroscopic strength improvements. However, this explanation was not investigated systematically or proven experimentally. Specifically, under the situation of the material under residual stress and external load, there are no reports of direct stress measurements or any direct observations of internal damage and failure processes. This was primarily due to the lack of an effective test method.

In recent years, micro-Raman spectroscopy has made substantial progress in stress testing of crystal materials including C fibre and SiC materials [11–14]. Scanning electron microscopes with in situ tensile testing apparatus have allowed significant revelations about material failure processes and mechanisms [15]. Using these advanced testing technologies and finite element simulation method, the aforementioned problem is herein comprehensively and systematically investigated. The microscopic mechanism behind the high-temperature macroscopic strength of C/SiC composites is revealed.

2 High-Temperature Strength Experiment of the C/SiC Composite

2.1 About the C/SiC Specimen

In the fabrication of C/SiC composite, the T300 carbon fiber bundles with a tow size of 1 k are prepared by 2D braided method into carbon cloth with the thickness of about 0.2 mm; then plain carbon clothes are stacked in parallel with voids are introduced. To enhance the desired non-linear/non-catastrophic tensile behaviour, the carbon fibres are coated with a pyrocarbon inter-phase of mean thickness 0.2 μm before infiltration by the matrix. After that, SiC matrix is deposited by chemical vapour infiltration method at 1273 K with the reactant gas of CH_3SiCl_3 . At this ambient condition, the density of the C/SiC composites is 2.05 g/cm^3 , and the volume fractions of carbon fibres, SiC matrix and voids are 42%, 44%, and 14%, respectively.

2.2 Experimental Design

To investigate variations in the C/SiC composite strength with temperature, a high-temperature experimental system is designed, as shown in Fig. 1. The furnace can reach up to 1100 °C. The maximum heating rate is 10 °C/min, and the temperature reaches 1000 °C in approximately 100 min. For convenience, the system employs a three-point bending method, as shown in Fig. 1b. The specimen base and pressure head are made of a SiC ceramic and are placed into the furnace. A 2 kN force sensor is connected to the pressure head, and circulating cooling water lowers the temperature and provides protection. The span between the two support points in the base is 30 mm. As shown in Fig. 1c, the specimen measures 40 × 10 × 2.5 mm and has an exterior oxidation protection layer of 30 μm . The ratio of the span to height of the specimen is 30: 2.5, which is larger than the commonly accepted standard for a slender beam (i.e. 10:1).

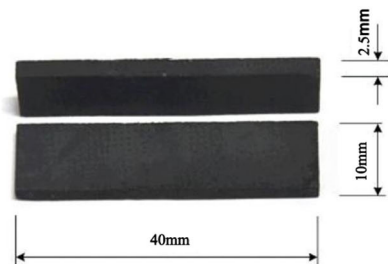
To investigate the variations in strength with temperature, the experiment temperature is set to room temperature, 550 °C, 700 °C, 900 °C and 1000 °C. After reaching each predefined temperature, the sample is maintained at that temperature for 10 min. Then, a load is applied continuously at a rate of 0.5 mm/min until the specimen fractures. Based on the load-time curve, a peak load is selected, and the bending strength of this specimen is calculated. At each temperature, 5 specimens are tested, and the average strength is used as the final result.



(a) High-temperature testing system



(b) High-temperature furnace observation window with a specimen inside



(c) Specimen dimensions

Fig. 1 High-temperature testing system and the specimen for measurement

2.3 Experiment Results

Figure 2 shows some typical loading curves and a summary of the material bending strengths at each temperature.

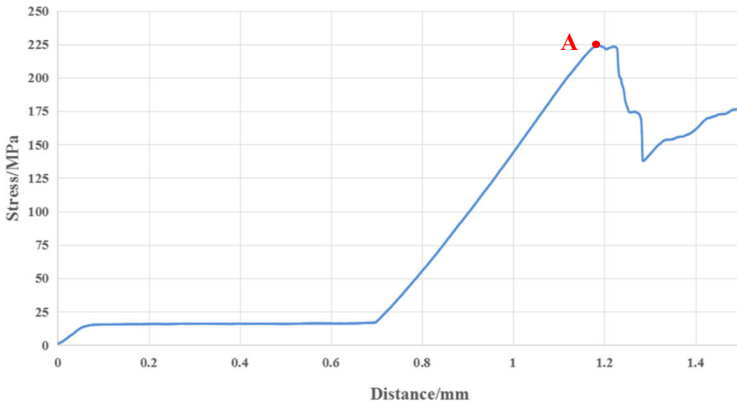
Between room temperature and 1000 °C, the bending strength of the C/SiC composite increases monotonously with increases of temperature. However, the fracture failure of the composite at high temperatures behaves more like a brittle fracture.

3 Observation of the Microscopic Failure of the C/SiC Composite Using Scanning Electron Microscopy with In Situ Loading

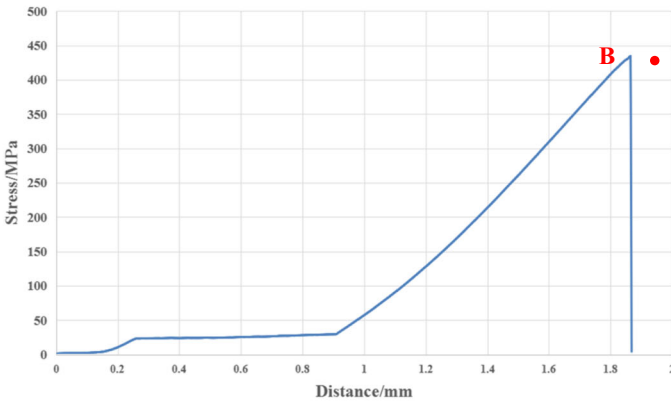
To understand the microscopic mechanism behind these changes in the macroscopic strength, the generation of internal fractures during failure is analysed using a scanning electron microscope with an in situ loading apparatus.

3.1 SEM In Situ Loading Experimental Design

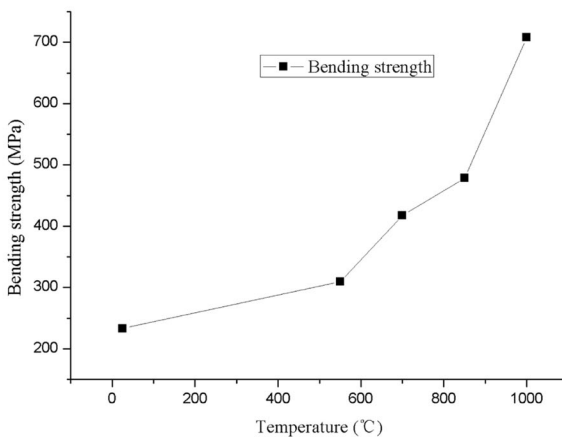
Scanning electron microscopy (SEM) with an in situ loading device, shown in Fig. 3, is used (Gatan MTEST5000, maximum load 5 kN, maximum temperature 600 °C). The specimen had dimensions of $12 \times 2 \times 3$ mm. The oxidation protection surface layer is removed by scraping to expose the smooth interior structure. In a temperature range of 25–500 °C, three-point bending



(a) Load-time curve showing an average bending strength of 233 MPa at room temperature



(b) Load-time curve showing an average bending strength of 417.7 MPa at 700°C



(c) a summary of the material bending strengths at each temperature

Fig. 2 Typical bending strength experiments covering various temperatures

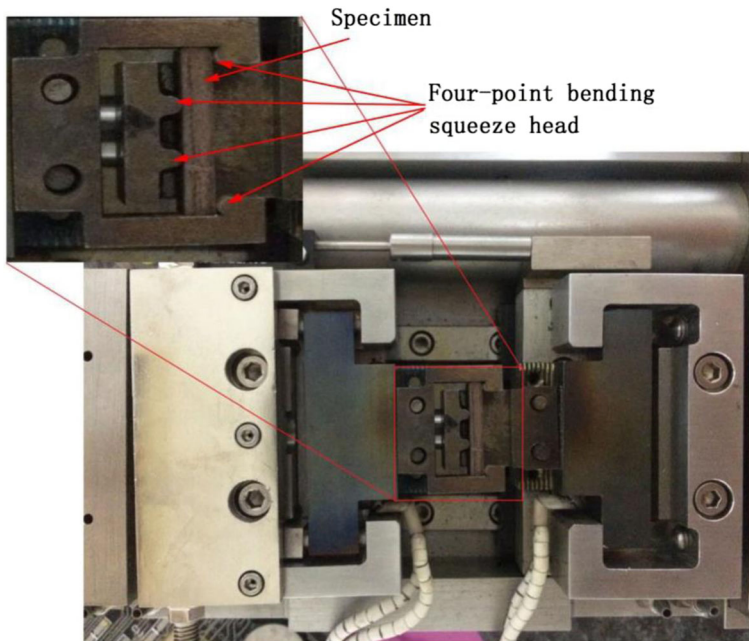


Fig. 3 The four-point bending fixture for in-situ test under SEM and the specimen

or four-point bending is applied. The load increases continuously at a rate of 0.5 mm/min. During this period, microscopic structural changes in the specimen are monitored, and the failure process and characteristics are recorded.

3.2 Experiment Results

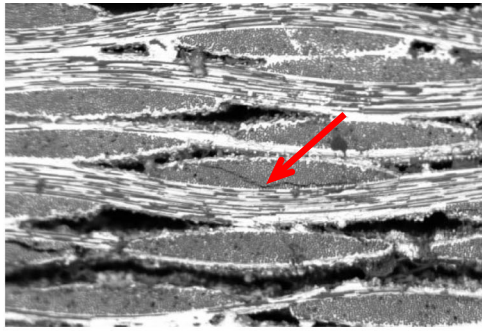
In situ loading at 500 °C shows that damage to the material always originates from vertical inter-fibre SiC matrix fracture, as shown in Fig. 4a, b. As the loading increases, the inter-fibre fracture expands rapidly to form a boundary layer between the horizontal and vertical fibres. Where one boundary fracture encounters another expanding boundary fracture opposite to the vertical fibre layer, the horizontal fibre layer is likely to rupture, as shown in Fig. 4c.

SEM of in-situ mechanical experiment shows that significant residual tensile stress may exist in the inter-fibre SiC matrix. The addition of an external load causes the matrix to reach its strength limit and rupture.

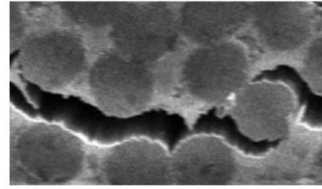
4 Micro-Raman Spectroscopy of C/SiC Residual Stress at Various Temperatures

4.1 Experiment Plan

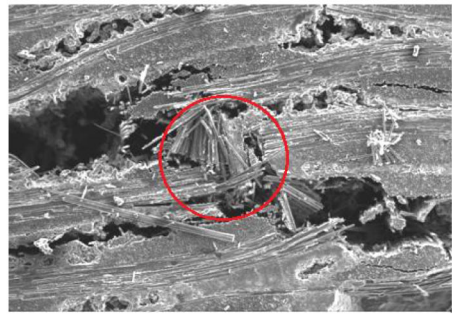
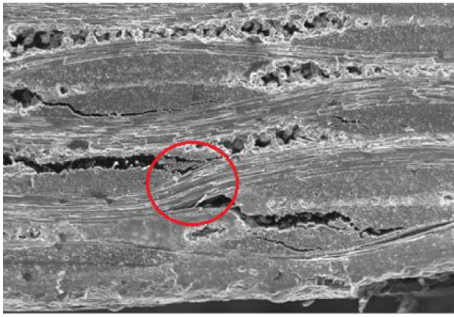
To directly investigate the tensile stress in the SiC matrix and its dependence on temperature, a focused ion beam (FIB) cold processing technique is employed to cut a small block of free-state SiC matrix material and a section of C fibre wrapped in SiC matrix material from the specimen (as shown in Fig. 5, approximately 28 μm long).



(a) Fracture origination between vertical fibres



(b) Enlarged image of a fracture



(c) Vertical inter-fibre fracture induced horizontal fibre rupture

Fig. 4 Matrix fracture origination and expansion

An HR-800 micro-Raman spectroscope (wavelength 532 nm, resolution approximately 1.72 cm^{-1}) is employed to perform a comparative experiment of the two specimens between 100 and 1200 cm^{-1} .

In the experiment, first, micro-Raman spectroscopy is employed to analyse the free-state SiC matrix at room temperature, $100\text{ }^{\circ}\text{C}$, $200\text{ }^{\circ}\text{C}$, $300\text{ }^{\circ}\text{C}$, $400\text{ }^{\circ}\text{C}$ and $500\text{ }^{\circ}\text{C}$. A sharp peak in spectrum and an offset with the temperature are used as references for the mechanical stress measurements to eliminate the influence of thermal factors. Then, the SiC specimen with C fibre-wrapped in is tested under identical conditions. The differences between two test results are compared to evaluate how the residual stress in the C fibre-wrapped SiC matrix varies with temperature.

4.2 Experiment Results

The Raman spectra of the free-state SiC matrix at room temperature and $500\text{ }^{\circ}\text{C}$ are shown in Fig. 6a. Both have a peak at 787 cm^{-1} that varies with temperature and is easy to identify. Details of this peak at six temperatures are shown in Fig. 6b. As the temperature increases, the peak position gradually shifts (from 787 cm^{-1} at room temperature to 775 cm^{-1} at $500\text{ }^{\circ}\text{C}$). Additionally, both the peak width and asymmetry increase.

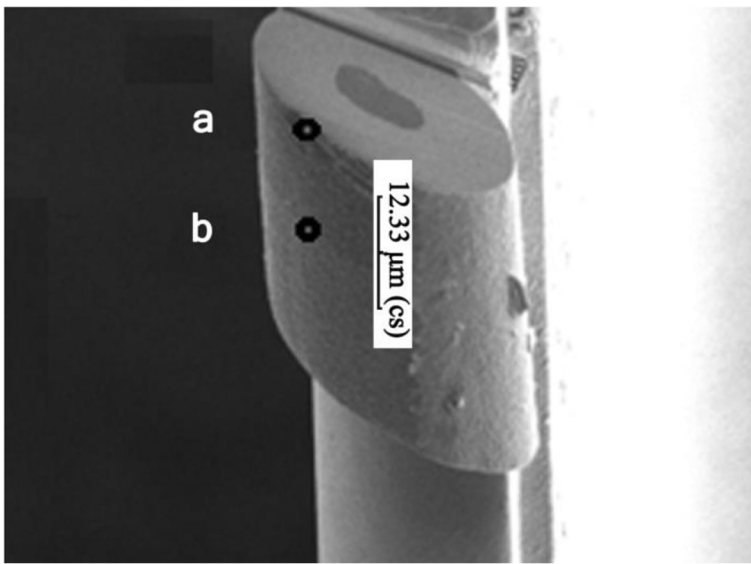
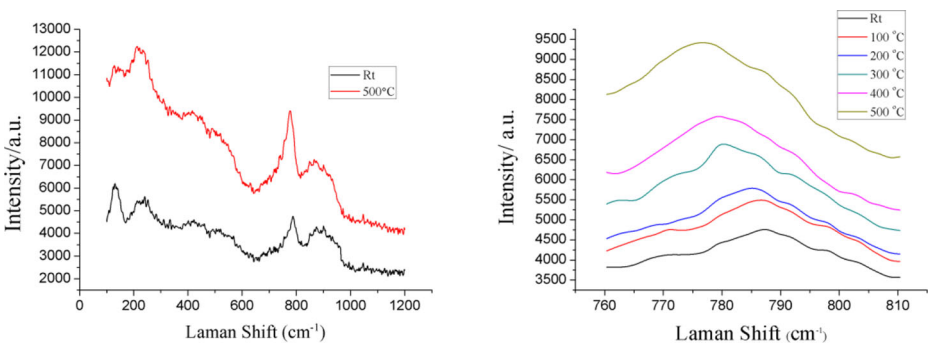


Fig. 5 Single C fibre specimen with SiC matrix cut using an FIB, the C fibre is the darker region in the middle

Micro-Raman spectroscopy is also performed for the two locations indicated on the side of the specimen in Fig. 5, and the results are shown in Fig. 7a. For convenience, only the range of 760–820 cm^{-1} is displayed. Using the peak position of the free-state matrix as a reference, the peak offsets of the SiC matrix wrapped around a C fibre at various temperature points are shown in Fig. 7b.

Compared with that of the free-state SiC matrix, the peak position of the SiC material around a C fibre barely changes with the temperature. However, the strength of the peak gradually increases, and the peak width increases symmetrically.

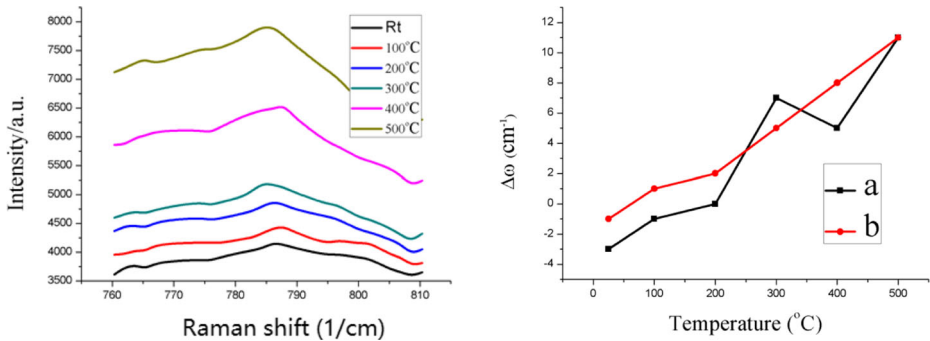
As the SiC matrix around a C fibre is in a complex stress state and as it is difficult to determine the effect of each stress component using the micro-Raman peak offsets, this experiment shows only that a mechanical stress exists in the SiC matrix around C fibres, mainly as axial and radial stress (whose signs are opposite).



(a) Complete spectra at room temperature and 500°C

(b) Variations in the peak near 787 cm^{-1} at 6 temperatures

Fig. 6 Raman spectra of the free-state SiC matrix



(a) Micro-Raman spectra of the diagnostic peak at various temperatures (b) Peak position shift vs. temperature

Fig. 7 Micro-Raman spectroscopy of the SiC matrix around a C fibre at various temperatures

5 Material Residual Stress Finite Element Analysis

The above experiment proves only that significant residual stress exists in the SiC matrix around the C fibres and that this stress is the key factor for composite material failure. However, understanding the quantitative distribution and variation of this residual stress with temperature requires comprehensive and accurate evaluation via a finite element calculation.

5.1 Finite Element Analysis Model

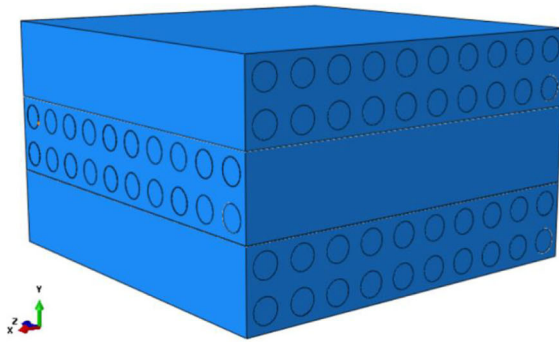
(1) Microscopic geometrical model of the C/SiC composite

The microscopic geometrical model has three layers. The first and the third layers are 0-degree fibre layers, and the middle layer is a 90-degree fibre layer. The fibre diameter is $d = 7 \mu\text{m}$, and the inter-fibre spacing is $a = 4 \mu\text{m}$. Each layer has a length of $110 \mu\text{m}$, a width of $110 \mu\text{m}$ and a height of $22 \mu\text{m}$. To simplify modelling, fibre inter-weaving is ignored, and the fibres are parallel to each other (Fig. 8a).

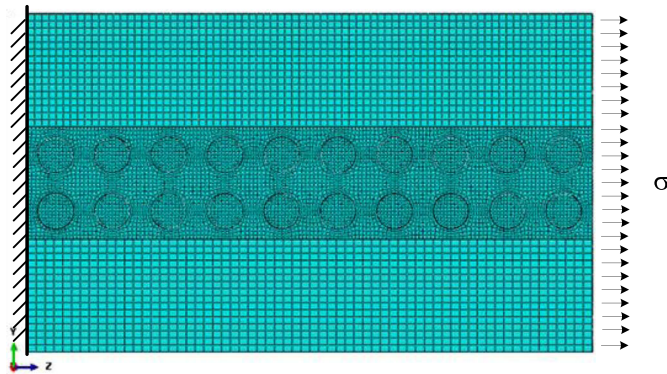
Due to the symmetry of the model, the finite element analysis is performed for half of the geometrical model. One face is used as the central symmetric plane to create boundary conditions; a uniformly distributed external load is applied on the opposite face. After meshing, the entire model contains 1,018,005 hexahedron units, as shown in Fig. 8b.

(2) C/SiC composite parameters

Parameters of the thermal analysis of the model are listed in Table 1. C fibre anisotropy is considered. Here, C fibre oxidation damage is not considered. Additionally, the mechanical properties of C fibre are assumed to not vary with temperature. The fibre moduli E_{f1} and E_{f3} are in-situ moduli that consider the effect of the high-temperature environment and the fibre bending on the properties of the fibre during preparation [16]. Furthermore, according to Z. Li [17, 18], the modulus E_m and thermal expansion coefficient of SiC matrix are basically independent on temperature.



(a) Microscopic geometrical model



(b) Meshing, load and boundary conditions; a total of 101×10^4 hexahedron units are present

Fig. 8 Microscopic geometrical model of the C/SiC composite and its load/boundary conditions

(3) Items in the finite element analysis

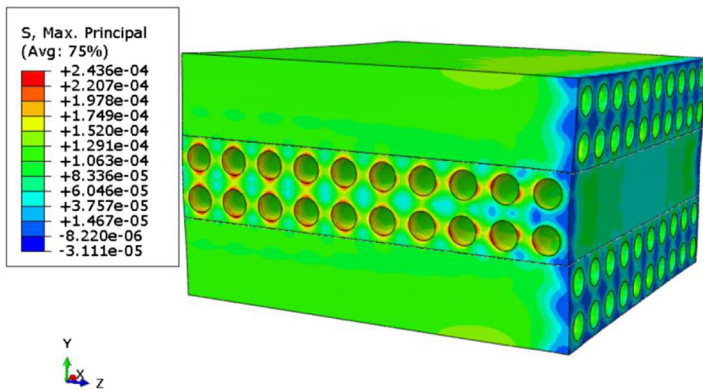
- A. The residual stress and variation of the interior of the material, particularly the SiC matrix, with temperature are the focus of the analysis. When the analysis is performed, the zero stress temperature is set to 1000 °C, and the external load is set to zero.
- B. The interior stress field distribution under residual stress and an external load (170 MPa).

Table 1 Material attributes of the fibre and matrix

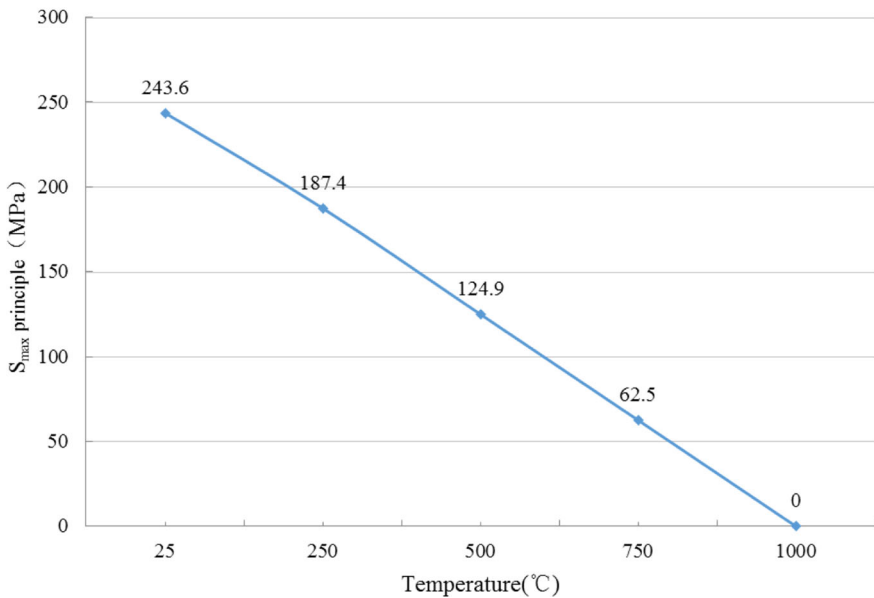
Radial elastic modulus of the fibre E_{f1}/GPa	Axial elastic modulus of the fibre E_{f3}/GPa	Elastic modulus of the matrix E_m/GPa	Poisson's ratio of the fibre ν_f	Poisson's ratio of the matrix ν_m
13.80	140.00	131.34	0.10	0.20
Shear modulus of the fibre G_f/GPa	Radial expansion coefficient of the fibre $\alpha_{f1}/\text{K}^{-1}\text{GH}$	Radial expansion coefficient of the fibre $\alpha_{f2}/\text{K}^{-1}$	Axial expansion coefficient of the fibre $\alpha_{f3}/\text{K}^{-1}$	Expansion coefficient of the matrix α_m/K^{-1}
4	8.80×10^{-6}	8.80×10^{-6}	9.00×10^{-7}	4.80×10^{-6}

5.2 Results of the Finite Element Analysis

Figure 9a shows the SiC matrix interior residual stress field (maximum principal stress) at room temperature. It shows that the SiC matrix around the C fibre has a maximum interior principal stress of 243.6 MPa. However, as temperature increases, the maximum interior principal stress of the SiC matrix gradually decreases, as shown in Fig. 9b.



(a) Maximum interior principal stress field distribution at room temperature of the SiC matrix (unit: 10^6 MPa)

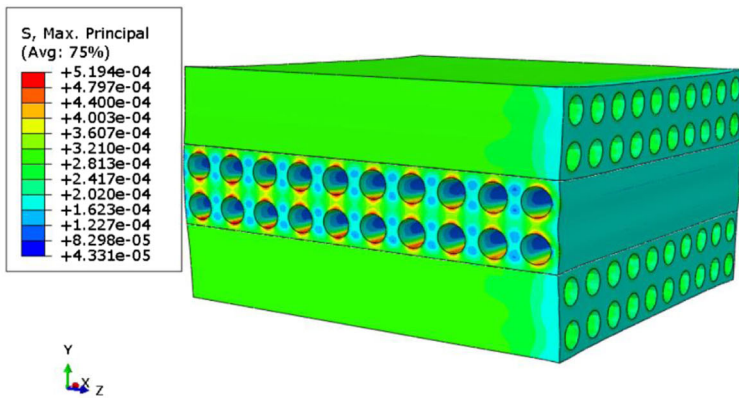


(b) Maximum interior residual principal stress of the SiC matrix versus temperature

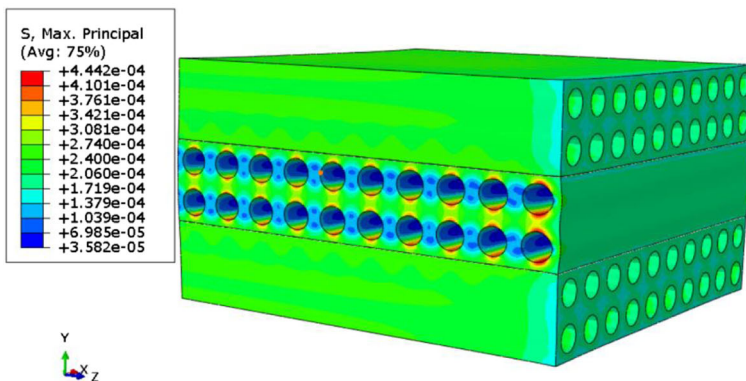
Fig. 9 Simulation results of the matrix interior residual stress of the SiC matrix and its variation with temperature

As predicted, under external loads (170 MPa) and residual stress, the maximum interior principal stress of the SiC matrix is strengthened. Figure 10a, b show simulation results of the interior maximum principal stress fields of the SiC matrix at room temperature and at 500 °C, respectively.

The simulation results shown in Fig. 10 reveal that significant maximum principal stress exists in the SiC matrix around the C fibres. The maximum interior principal stress of the SiC matrix at room temperature is 80 MPa larger than that at 500 °C. Apart from the thermal mismatch between the SiC matrix and the C fibre, another important factor is the small in-plane elastic modulus of the C fibre, which is likely to concentrate stress in the surrounding SiC matrix. Due to the extremely high C fibre strength and the decreasing residual stress in the SiC matrix as the temperature increases, external load always causes fractures to originate from the inter-fibre matrix. Additionally, higher temperatures require larger external loads to reach the ultimate stress of the SiC matrix. This model is a reasonable explanation for the increasing macroscopic strength of this material.



(a) Maximum principal stress field at room temperature (unit: 10⁶ MPa)



(b) Maximum principal stress field at 500°C (unit: 10⁶ MPa)

Fig. 10 Maximum interior principal stress field of the SiC matrix under external load and residual stress

6 Conclusions and Final Remarks

In this study, mechanical experiment and finite element calculations are combined to systematically investigate the macroscopic strength behaviour of a C/SiC composite and its underlying microscopic physical mechanism. This study provides a basis to further improve the manufacturing process and macroscopic mechanical properties of C/SiC composites.

The following conclusions are reached through this investigation:

- (1) High-temperature experiment shows a monotonic increase in the C/SiC composite strength with temperature.
- (2) SEM with in situ bending experiment proves that during loading, fractures in the C/SiC composite always originate from the horizontal inter-fibre SiC matrix and rapidly expand to the horizontal and vertical fibre boundaries. Thus, the SiC matrix is the weak point of composite.
- (3) Micro-Raman spectroscopy proves that residual stress exists in the SiC matrix.
- (4) A finite element method quantitatively is used to calculate the residual stress in the SiC matrix and proves that as the temperature increases, the residual stress decreases almost linearly. Under residual stress and external load, significant tensile stress exists in the SiC matrix around the C fibres. Failure is likely to occur at this location, which matches the results of the microscopic mechanical experiment.

The above conclusions provide a reasonable explanation for the increase in C/SiC composite strength with temperature: residual tensile stress in brittle SiC matrix material plays a pivotal role in material failure process. Under residual tensile stress and an external tensile load, the matrix around the C fibres is the first to reach its ultimate stress and fail, which quickly leads to catastrophic material rupture. However, residual stress in the SiC matrix is decreased as temperature increases. The result is that the ultimate stress of the material is only reached under larger external loads, increasing the material strength at the macroscopic level.

Although the high-temperature strength behaviour of the C/SiC composites and the underlying microscopic mechanism are revealed, constraints on the experiment conditions and technical capabilities cause two issues that should be investigated further to ensure more reliable conclusions:

- (1) Micro-Raman spectroscopy only provides the residual stress of the SiC matrix, but this stress cannot be isolated, and there is no explanation for why peak does not vary with temperature.
- (2) The dependence of the mechanical properties of the SiC matrix on temperature is not well understood, which may affect the precision of the finite element simulation.

Acknowledgements The authors appreciate sponsorship from the National Natural Science Foundation of China (11672340) for supporting this research. In addition, the authors declare that no conflict of interest exists in the submission of this manuscript.

References

1. Yang, Y., Xu, F., Gao, X., et al.: Impact resistance of 2D plain-woven C/SiC composites at high temperature. *Mater. Des.* **90**, 635–641 (2016)
2. Choury, J.J., Thermostructural composite materials: Fabrication and main applications. In: proceedings of the 4th international symposium on ceramic materials and components for engines. In: Chapman and Hall London: 102–112 (1992)
3. Heraud, L., Spriet, P.: High toughness C/SiC and SiC/SiC composites in heat engines, Whisker- Fiber-Toughened Ceram, pp. 217–224 (1988)
4. Feldhoff, A., Pippel, E., Woltersdorf, J.: Interface engineering of carbon fiber reinforced Mg–Al alloys. *Adv. Eng. Mater.* **2**(8), 471–480 (2000)
5. Pimenta, S., Pinho, S.T.: Recycling carbon fibre reinforced polymers for structural applications: technology review and market outlook. *Waste Manag.* **31**, 378–392 (2011)
6. Engesser J M. Monotonic, creep-rupture, and fatigue behavior of carbon fiber reinforced silicon carbide (C/SiC) at an elevated temperature [J]. 2004
7. Luan, X., Cheng, L., Xie, C.: Stressed oxidation life prediction of 3D C/SiC composites in a combustion wind tunnel[J]. *Compos. Sci. Technol.* **88**, 178–183 (2013)
8. Cao, X., Yin, X., Fan, X., et al.: High-temperature flexural properties of SiBC modified C/SiC composites [J]. *Ceram. Int.* **40**(4), 6185–6190 (2014)
9. Yang, C.P., Zhang, L., Wang, B., et al.: Tensile behavior of 2D-C/SiC composites at elevated temperatures: experiment and modelling [J]. *J. Eur. Ceram. Soc.* (2016)
10. Patel, M., Kiran, M.P.S., Kumari, S., et al.: Effect of oxidation and residual stress on mechanical properties of SiC seal coated C/SiC composite [J]. *Ceram. Int.* **44**(2), 1633–1640 (2018)
11. Wolf, I.D., Maes, H.E., Jones, S.K.: Stress measurements in silicon devices through Raman spectroscopy: Bridging the gap between theory and experiment [J]. *J. Appl. Phys.* **79**(9), 7148–7156 (1996)
12. Young, R.J., Huang, Y.L., Gu, X., et al.: Analysis of composite test methods using Raman spectroscopy. *Plastics, Rubber & Composites Processing and Appl.* (23), 11–19 (1995)
13. Wolf, I.D., Jian, C., Spengen, W.M.V.: The investigation of microsystems using Raman spectroscopy [J]. *Opt Lasers Eng.* **36**(2), 213–223 (2001)
14. Ghosh, D., Subhash, G., Orlovskaya, N.: Measurement of scratch-induced residual stress within SiC grains in ZrB₂–SiC composite using micro-Raman spectroscopy [J]. *Acta Mater.* **56**(18), 5345–5354 (2008)
15. Liu, X., Liu, Y., Jin, B., et al.: Microstructure evolution and mechanical properties of a sintered mg alloy under in situ SEM tensile testing [J]. *J Mater Sci Technol.* **33**(3), 224–230 (2017)
16. Zhang, L.T.: Fiber-reinforced silicon carbide ceramic composites: modelling, characterization and design. Chemical Industry Press, Beijing (2009)
17. Li, Z., Bradt, R.C.: Thermal expansion of the cubic (3C) polytype of SiC. *J. Mater. Sci.* **21**, 4366–4368 (1986)
18. Li, Z., Bradt, R.C.: The single crystal elastic constant of cubic (3C) SiC to 1000 °C. *J. Mater. Sci.* **22**, 2257–2259 (1987)

Publisher's Note Springer Nature remains neutral with regard to jurisdictional claims in published maps and institutional affiliations.